The Stellar Contribution to the Extragalactic Background Light: Implications for Propagation of Ultra High Energy Cosmic Rays and TeV Gamma Rays

Soebur Razzaque*† Justin D. Finke*†, Charles D. Dermer*

*U.S. Naval Research Laboratory, Code 7653, 4555 Overlook Ave SW, Washington, DC, 20375-5352, USA
†NRL/NRC Resident Research Associate

***Abstract*. We present models of extragalactic background light (EBL) from the infrared to ultraviolet derived from the stellar initial mass function, star formation history of the universe, and absorption of ultraviolet photons by dust and reemission in infrared. These models are simultaneously fitted to the EBL data as well as to the data on the stellar luminosity density. We discuss implications of our results for the propagation of ultrahigh-energy cosmic rays and TeV gamma rays from their sources to Earth in the EBL, and a calculation of the gamma- ray horizon for UHECR protons. The results are applied to the highest energy photons observed from extragalactic sources measured with the Fermi Gamma ray Space Telescope.**

***Keywords*: diffuse radiation — gamma-rays — cosmic rays**

I. INTRODUCTION

The extragalactic background light (EBL) from the far infrared through the visible and extending into the ultraviolet is thought to be dominated by starlight, either through direct emission or through absorption and reradiation by dust. Direct measurement of the EBL is difficult (see [1] for a review) due to contamination by foreground zodiacal and Galactic light. Galaxy counts may also be used to estimate the EBL, but the unknown number of unresolved sources results in a lower limit. The general picture is a component peaking at around 1 μm from direct starlight emission and one peaking at $\sim$ 100 μm from re-emission of absorbed starlight by dust. Due to different modeling approaches and uncertainties in underlying model parameters, the intensity and shape of the EBL spectrum remains controversial. The EBL absorbs γ-rays from distant sources, creating electron-positron pairs, and is thus an important radiation field for γ-ray astronomy.

Interactions between the cosmic microwave background (CMB) and the highest energy cosmic ray protons and/or ions lead to the Greisen-Zatsepin-Kuzmin (GZK) cutoff through photohadronic processes. The far-IR to UV EBL is also important for the propogation of cosmic rays, although less so than the CMB.

In this proceeding, we summarize recent results of our modeling of the EBL (§ II), and apply this model to interactions with γ-rays (§ III) and cosmic rays (§ IV).

II. MODELING THE EBL FROM STARS AND DUST

We have modeled the EBL from stars and dust ([2], [3], hereafter RDF09 and FRD09 respectively). The comoving stellar luminosity density is given by

$$\epsilon\, j^{stars}(\epsilon; z) = \epsilon^2 f_{esc}(\epsilon) \int_{m_{min}}^{m_{max}} dm\ \xi(m) \times \dot{N}_\star(\epsilon; m, t_\star(z)) \int_z^{z_{max}} dz_1 \left|\frac{dt_*}{dz_1}\right| \psi(z_1) \qquad (1)$$

where ϵ is the dimensionless photon enegy, m is the stellar mass normalized to the solar mass, f_{esc} is the fraction of starlight that escapes extinction by dust, $\xi(m)$ is the initial mass function (IMF), $\psi(z)$ is the star formation rate (SFR), $\dot{N}_\star(\epsilon; m, t_\star(z))$ is the stellar photons emitted per unit time, and $t_\star$ is the age of the star. The stars are assumed to be blackbodies and the formulae of Eggleton et al. [4] are used to determine the stellar temperature, radius, and luminosity as the stars evolve on the main sequence, the Hertzsprung gap, the giant branch, the horizontal branch, the asymptotic giant branch, and the white dwarf stage. The dust absorption model from Driver et al. [5] is used for $f_{esc}(\epsilon)$. Once the stellar component is calculated, the dust constribution to the luminosity density is calculated self-consistently,

$$f_n \int d\epsilon\, \frac{1}{f_{esc}(\epsilon)} [1 - f_{esc}(\epsilon)] j^{stars}(\epsilon; z) = \int d\epsilon\, j_n(\epsilon; \Theta_n)\ , \qquad (2)$$

where f_n is the fraction of the absorbed emissivity reradiated in a particular dust component, $\Theta_n = k_{\rm B} T_n / m_e c^2$ is the dimensionless temperature of the dust component, and the subscripts n =1, 2, and 3 refer to the warm large dust grains, hot small dust grains, and polycyclic aromatic hydrocarbons, respectively. This EBL model has 8 free parameters: $\psi(z)$, $\xi(m)$, Θ_n, and f_n with $n = 1, 2, 3$. The IMF and SFR are further constrained by the collection of SFR data from [6]. These parameters are determined through fits to a variety of luminosity density data between $z = 0$ and $z = 3$. The results are the SFR, $\psi(z)$ from Hopkins & Beacom [6] fit with the smooth parameterization of Cole et al. [7], the IMF, $\xi(m)$ of Baldry & Glazebrook [8], and the dust parameters given in Table I.

Once the luminosity density has been calculated at a variety of redshifts, the proper EBL energy density can

TABLE I
DUST PARAMETERS. SEE TEXT FOR DETAILS.

Component	n	f_n	T_n [K]	Θ_n [10^{-9}]
Warm Large Grains	1	0.60	40	7
Hot Small Grains	2	0.05	70	12
PAHs	3	0.35	450	76

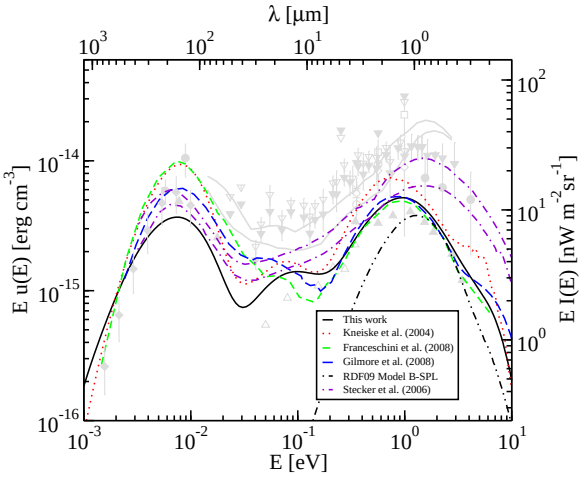

Fig. 1. EBL energy density for our two models (labeled "This model" and "RDF09 Model B-SPL"), including the one presented in this proceeding, along with several EBL measurements and constraints (grey lines and points) derived from TeV blazar data.

be calculated,

$$\epsilon'' \, u''_{EBL}(\epsilon'';z) = (1+z)^4 \int_z^{z_{max}} dz_1 \, \frac{\epsilon'' j_{\epsilon''}(z_1)}{(1+z_1)} \left| \frac{dt_*}{dz_1} \right| , \quad (3)$$

where

$$\epsilon'' = \frac{1+z_1}{1+z} \epsilon \, ,$$

and

$$\epsilon'' \, j_{\epsilon''}(z) = \epsilon'' \, j^{stars}_{\epsilon''}(z) + \epsilon'' \, j^{dust}_{\epsilon''}(z)$$

is the total comoving luminosity density. The relationship between the cosmic time and redshift in a flat ΛCDM universe is $dt/dz = -1/[H_0(1+z)\sqrt{\Omega_m(1+z)^3+\Omega_\Lambda}]$. The EBL energy density for our model, and the models of several other authors ([9], [10], [11], [2], [12]) is presented in Fig. 1, along with several EBL measurements and lower limits from galaxy counts (upward pointing triangles) and upper limits from blazar observations (downward pointing triangles and grey lines). Our model is very close to the models of [10] and [11] in the near-IR to UV, although below their models in the far-IR. Our model is generally below the direct measurements (e.g., [13], [14], [15] but consistent with the upper limits from γ-ray observations of blazars ([16], [17]) and very near the lower limits from galaxy counts. In one notable case, it is slightly below the lower limit [18]. Since our model is consistent with the luminosity density measurements, this indicates some discrepency between luminosity density and EBL measurements.

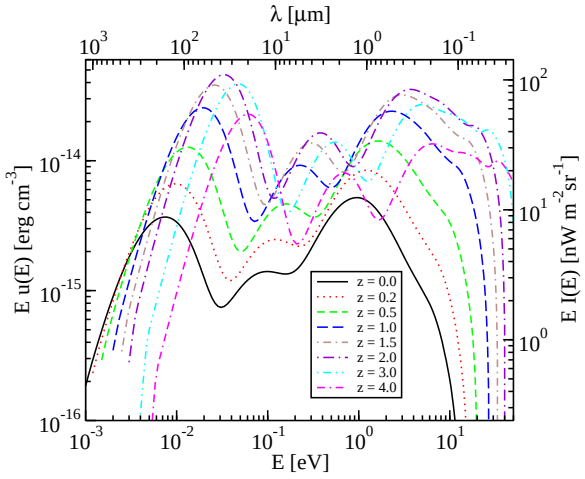

Fig. 2. The proper EBL energy density as a function of proper photon energy for our model, for a variety of redshifts. We use this EBL evolving with redshift to calculate the $\gamma\gamma \to e^+e^-$ absorption opacity in Eq. (4).

Fig. 2 shows the redshift evolution of our model. This peaks at around $z \approx 2$, which is about where the SFR peaks (see RDF09 and FRD09). Also note that at higher redshifts, there are more high mass stars to create a larger high energy component. The high z SEDs are flatter in the optical-UV due to this relatively higher contribution of high mass stars. At lower z, the contribution is greater from longer living low mass stars, as well as those high mass stars which have evolved off the main sequence. This also affects the dust emission component. At around $z = 1$ the far-IR dust component peaks at a greater energy density than does the optical stellar component, and the mid-IR PAH component gets progressively greater at higher z. Since the dust absorption is greater at higher energy (lower wavelength), where the high mass stars emit most of their radiation, the absorption is greater at higher z, and thus the dust emission is greater at higher z.

III. ABSORPTION OF GAMMA-RAYS

The far-IR to UV EBL is the most important radiation field for photons with energy ϵ_1(TeV) interacting with long-wavelength photons with and absorbing γ-rays from distant sources, with the threshold $\gamma\gamma$ condition implying that

$$\epsilon_1(TeV) = \frac{0.26}{(1+z)\,\epsilon_{EBL}(eV)} \, .$$

The absorption optical depth of γ-ray photons as a function of observed γ-ray photon energy, ϵ_1, can be calculated by

$$\tau_{\gamma\gamma}(\epsilon_1,z) = \frac{c\pi r_e^2}{\epsilon_1^2 m_e c^2} \int_0^z \frac{dz'}{(1+z')^2} \left| \frac{dt_*}{dz'} \right| \times \int_{\frac{1}{\epsilon_1(1+z')}}^{\infty} d\epsilon'' \frac{\epsilon'' u''_{EBL}(\epsilon'';z')}{\epsilon''^4} \, \bar{\phi}(\epsilon'' \epsilon_1 (1+z')) \, , \quad (4)$$

with the EBL energy density evolving with redshift. The function $\bar{\phi}$ is given in Refs. [19], [20]

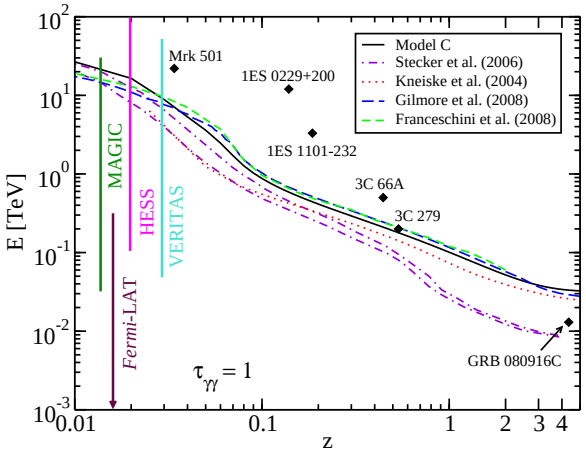

Fig. 3. A plot of $\tau_{\gamma\gamma} = 1$ for several EBL models including our model C, as a function of redshift. Curves signify the same models as in Fig. 1. Also plotted by the filled diamonds are the maximum γ-ray photon energy bins from blazars observed with atmospheric Cherenkov telescopes and the GRB 080916C observed with the large area telescope (LAT) onboard the *Fermi* gamma-ray space telescope.

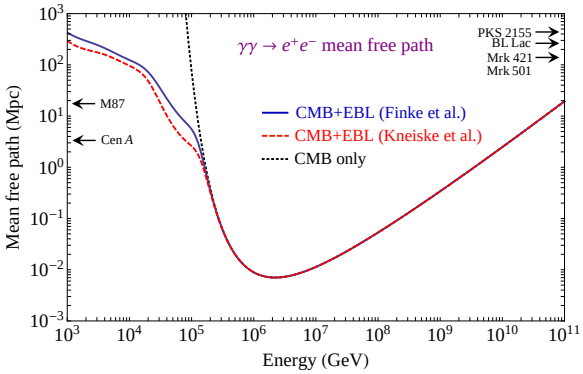

Fig. 4. The mean-free-path of high-energy γ ray absorption with the CMB and EBL photons in the nearby universe. The Knesike et al. [9] and Finke et al. [3] EBL models give the most and least intense EBL at $\sim$ 100 μm, respectively. A diffuse radio background (not shown here) may dominate the $\gamma\gamma$ *mfp* above 10^{10} GeV. Also shown are the distance scale for nearby prominent AGNs.

A Fazio-Stecker [21] plot of the energy at which the universe becomes optically thick to γ-rays, the curve where $\tau_{\gamma\gamma} = 1$, is given in Fig. 3 for several models, including our model. Also plotted are the maximum photon energy bin of several blazars, observed with atmospheric Cherenkov telescopes (see [17] for a list and references) and the GRB 080916C [22] observed with Fermi gamma ray space telescope. The VHE γ-rays from many blazars are highly attenuated by the EBL, since several are considerably above the $\tau_{\gamma\gamma} = 1$ curve for all models. Also note that the universe will be optically thin to 20 GeV and lower photons over all redshifts for all models except those of [12].

The absorption of γ-rays from distant blazars can be used to put upper limits on the EBL (e.g., [23], [24], [16], [17]). However, the lack of consensus on the intrinsic spectra of blazars has led to considerable controversy on these limits (e.g., [25], [26]). Also, the detection of a 13 GeV photon from the GRB 080916C at z=4.35 [22] gives a tantalizing, although certainly not conclusive, clue to the EBL at high z.

Gamma rays created from the $\pi^0 \rightarrow \gamma\gamma$ processes by UHECRs, either interacting at their sources or in the CMB and EBL background, can induce electromagnetic cascade via e^+e^- pair production and Compton scattering of background photons by these electrons and positrons [27], [28], [29]. A synchrotron radiation component by e^+e^- pairs can also contribute if the intergalactic magnetic field is of the order of 1 nG [30]. The interaction mean-free-path (*mfp*) for $\gamma\gamma \rightarrow e^+e^-$ is dominated by the CMB for $\epsilon > 200$ TeV (see Fig. 4), and is given by $\lambda_{\gamma\gamma,CMB} \simeq 2(\epsilon/\mathrm{PeV})/\ln[0.4\epsilon/\mathrm{PeV}]$ kpc for $\epsilon \gg$ PeV [29]. Figure 4 shows the $\gamma\gamma$ *mfp* with the CMB and EBL photons. The EBL model by Kneiske et al. [9] is one of the two models producing the most intense emission at 100μm (see Fig. 1) and the model by FRD09 produces the least intense emission at the same wavelength. We used these two models in Fig. 4 as two extreme cases. The contribution by the EBL to $\lambda_{\gamma\gamma}$ dominate for $\epsilon < 200$ TeV.

The e^+e^- pairs upscatter CMB photons in the Klein-Nishina regime for $\gamma_e \gg 10^{10}$ with a *mfp* $\lambda_{KN} \simeq 2.1(\gamma_e/10^9)/[\ln(1.8\gamma_e/10^9) - 2]$ kpc, and in the Thomson regime for $\gamma_e \ll 10^9$ with a *mfp* of $\lambda_T \simeq 7.5 \times 10^8/\gamma_e$ kpc [29]. The e^+e^- pairs however are subject to deflection in the intergalactic magnetic field, the strength of which is not well constrained. An electron with Larmor radius r_L is deflected by an angle $\theta_d \simeq \lambda_{T/KN}/r_L$ before it upscatters a CMB photon. Thus for a source with relativistic jet of opening angle $\theta_{jet} > \theta_d$, electromagnetic cascade emission can be identified with the source as a hard γ-ray component. Cascade emission from sources such as nearby AGNs could be detectable with current and upcoming Cherenkov telescopes if the intergalactic magnetic field is $< 10^{-12}$ G.

IV. The EBL and Cosmic Rays

UHECR protons interact with the CMB and EBL photons, and lose energy while propagating from their sources to us. The dominant energy loss channels are the Bethe-Heitler pair production $p\gamma \rightarrow pe^+e^-$, and photopion production $p\gamma \rightarrow n\pi^+/p\pi^0$. The mean-free-path for these energy loss processes, with an energy loss rate of dE/dt, is given by

$$r_{mfp}(E) = \frac{cE}{|dE/dt|}, \tag{5}$$

at low redshift. An UHECR horizon pathlength, on the other hand, is defined as the average distance over which its measured energy E has dropped from an initial energy eE and is given by [29]

$$r_{hrz}(E) = \int_E^{eE} \frac{dE}{E} r_{mfp}(E). \tag{6}$$

Figure 5 shows the *mfp* and horizon pathlengths for UHECR protons in the CMB only, and in the CMB with

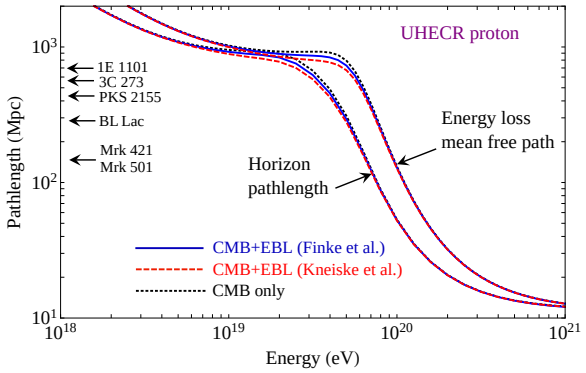

Fig. 5. The energy loss mean-free and horizon pathlengths of the UHECR proton propagation in the CMB and EBL models. The horizon path length is defined in Eq. (6) as the integrated *mfp* in Eq. (5) over which the energy of an UHECR with observed energy E starts with an energy eE. The horizon pathlength is 50 Mpc, 100 Mpc and 200 Mpc respectively for 100 EeV, 80 EeV and 60 EeV protons. The differences in EBL models are evident in the horizon pathlength at 10–40 EeV. Also shown are the distance scale for nearby prominent AGNs.

Finke et al. [3] or Kneiske et al. [9] EBL model. To calculate the photopion losses by UHECR protons, we used a $p\gamma$ cross-section times the mean energy loss factor by protons as $\sigma_0 = \sigma_{p\gamma} \approx 68$ μb and we take a pion-production threshold energy of 0.2 GeV in the rest frame of the proton [31]. To calculate the Bethe-Heitler e^+e^- pair production losses by UHECR protons, we used formulae in Refs. [32], [33]. The horizon pathlength for 10^{20} eV proton is 50 Mpc, for 8×10^{19} eV proton is 100 Mpc, and that for 6×10^{19} eV proton is 200 Mpc. The sources of UHECR protons with $E > 6 \times 10^{19}$ eV thus need to be within a distance < 200 Mpc, which is consistent with clustering observed in the Pierre Auger data, above this energy, with the super-galactic plane on ≥ 75 Mpc scales.

The horizon pathlength above 4×10^{19} eV is dominated by the photopion energy losses with the CMB. In the 10^{18} eV – 4×10^{19} eV range Bethe-Heitler photopair with the CMB dominates the energy losses, however photopion with the EBL results in different horizon lengths for different EBL models in this energy range. Thus predictions for UHECR induced cascades producing GeV–TeV γ rays and PeV neutrinos depend on the EBL models. A search for such emission with the *Fermi* gamma ray space telescope, ground-based Cherenkov telescopes such as HESS, MAGIC, VERITAS and HAWC, and the neutrino telescopes such as IceCube and KM3NeT from nearby known AGNs could be revealing if they are the sources of UHECRs.

V. Conclusion

We have reported on our recently developed EBL model in the 0.001–10 eV range using direct and reprocessed stellar radiation. Our EBL model is mostly consistent with the EBL lower limits derived from galaxy counts, and is also consistent with stellar luminosity density data at various redshifts. We properly take into account redshift evolution of our EBL model which is important for calculating absorption optical depth of high energy photons from distant astrphysical sources to interact with EBL photons. The opacity we have calculated is consistent with data from TeV blazars. High-energy γ-rays, directly from the astrophysical sources, that are absorbed by the CMB and EBL can induce an electromagnetic cascade by Compton scattering CMB photons. UHECR protons that lose energy by producing neutral pions will also induce electromagnetic cascades. A hard γ-ray component from these cascades can be searched for indications of UHECR acceleration from the directions of the astrophysical objects. Propagation of 10^{19} eV – 4×10^{19} eV protons is affected by the EBL and the effect is smallest for our EBL model.

Acknowledgements

This work was supported by the Office of Naval Research and GLAST Science Investigation DPR-S-1563-Y, and by NASA Swift Guest Investigator Grant DPR-NNG05ED41I.

References

[1] Hauser, M. G. & Dwek, E. 2001, *ARA&A*, 39, 249
[2] Razzaque, S., Dermer, C. D., & Finke, J. D. 2009, *ApJ*, 697, 483
[3] Finke, J. D. Razzaque, S., & Dermer, C. D., 2009, *ApJ*, submitted, arXiv:0905.1115
[4] Eggleton, P. P., Tout, C. A., & Fitchett, M. J. 1989, *ApJ*, 347, 998
[5] Driver, S. P., Popescu, C. C., Tuffs, R. J., Graham, A. W., Liske, J., & Baldry, I. 2008, *ApJ*, 678, L101
[6] Hopkins, A. M. & Beacom, J. F. 2006, *ApJ*, 651, 142
[7] Cole, S. et al. 2001, *MNRAS*, 326, 255
[8] Baldry, I. K. & Glazebrook, K. 2003, *ApJ*, 593, 258
[9] Kneiske, T. M., Bretz, T., Mannheim, K., & Hartmann, D. H. 2004, *A&A*, 413, 807
[10] Franceschini, A., Rodighiero, G., & Vaccari, M. 2008, *A&A*, 487, 837
[11] Gilmore, R. C., Madau, P., Primack, J. R., & Somerville, R. S. 2008, in American Institute of Physics Conference Series, Vol. 1085, American Institute of Physics Conference Series, 577–580
[12] Stecker, F. W., Malkan, M. A., & Scully, S. T. 2006, *ApJ*, 648, 774
[13] Bernstein, R. A., Freedman, W. L., & Madore, B. F. 2002, *ApJ*, 571, 56
[14] Bernstein, R. A. 2007, *ApJ*, 666, 663
[15] Levenson, L. R., Wright, E. L., & Johnson, B. D. 2007, *ApJ*, 666, 34
[16] Mazin, D. & Raue, M. 2007, *A&A*, 471, 439
[17] Finke, J. D. & Razzaque, S. 2009, *ApJ*, in press, arXiv:0904.2583
[18] Levenson, L. R. & Wright, E. L. 2008, *ApJ*, 683, 585
[19] Gould, R.J. & Shréder, G. 1967, *Phys. Rev.*, 155, 1404
[20] Brown, R.W., Mikaelian, K.O. & Gould, R.J. 1973, Astrophysical Letters, 14, 203
[21] Fazio, G. G. & Stecker, F. W. 1970, *Nature*, 226, 135
[22] Abdo, A. A. et al. 2009, Science, 323, 1688
[23] Stecker, F. W. & de Jager, O. C. 1993, *ApJ*, 415, L71
[24] Aharonian, F. et al. 2006, *Nature*, 440, 1018
[25] Stecker, F. W., Baring, M. G., & Summerlin, E. J. 2007, *ApJ*, 667, L29
[26] Böttcher, M., Dermer, C. D., & Finke, J. D. 2008, *ApJ*, 679, L9
[27] Waxman, E., & Coppi, P. 1996, *ApJ*, 464, L75
[28] Razzaque, S., Mészáros, P., & Zhang, B., 2004, *ApJ*, 613, 1072
[29] Dermer, C.D., Razzaque, S., Finke, J.D., & Atoyan, A. 2009, *New J. Phys.*, accepted, arXiv:0811.1160
[30] Gabici, S., & Aharonian, F. 2005, *Phys. Rev. Lett.*, 95, 251102
[31] Dermer, C. D. 2007, *ApJ*, 664, 384
[32] Blumenthal, G. 1970, *Phys. Rev.*, D1, 1596
[33] Chodorowski, M., et al. 1992, *ApJ*, 400, 181